Equilibrium roughening transition in a one-dimensional modified sine-Gordon model

Saúl Ares*

*Grupo Interdisciplinar de Sistemas Complejos (GISC) and Departamento de Matemáticas, Universidad Carlos III de Madrid,
Avenida de la Universidad 30, 28911 Leganés, Madrid, Spain*

Angel Sánchez†

*Grupo Interdisciplinar de Sistemas Complejos (GISC) and Departamento de Matemáticas, Universidad Carlos III de Madrid,
Avenida de la Universidad 30, 28911 Leganés, Madrid, Spain*
and Instituto de Biocomputación y Física de Sistemas Complejos, Universidad de Zaragoza, 50009 Zaragoza, Spain

We present a modified version of the one-dimensional sine-Gordon model that exhibits a thermodynamic, roughening phase transition, in analogy with the two-dimensional usual sine-Gordon model. The model is suited to study the crystalline growth over an impenetrable substrate and to describe the wetting transition of a liquid that forms layers. We use the transfer integral technique to write down the pseudo-Schrödinger equation for the model, which allows us to obtain some analytical insight, and to compute numerically the free energy from the exact transfer operator. We compare the results with Monte Carlo simulations of the model, finding a perfect agreement between both procedures. We thus establish that the model shows a phase transition between a low-temperature flat phase with intriguing nontrivial properties and a high-temperature rough one. The fact that the model is one-dimensional and that it has a true phase transition makes it an ideal framework for further studies of roughening phase transitions.

PACS number(s): 81.15.Aa, 68.35.Ct, 68.35.Rh, 05.40.$-$a

I. INTRODUCTION

The two-dimensional (2D) ordered sine-Gordon model is today a fairly well understood problem (see, e.g., [1–6]). However, the random version of the model, where quenched disorder is introduced, is far less understood and still subject to discussion. Since the *super-roughening* transition (see Sec. II below for a definition) was introduced in 1990 [7], there has been no theoretical agreement about its nature and the properties of the super-rough phase (see [8] for a review, see [9] for more references). Large-scale numerical simulations or exact optimization results [10–18] were not enough to solve the question, due to its highly demanding computational character. To circumvent this problem, in [19] we proposed a modification of the 1D model, in order to have a less demanding problem that could give us information about the super-rough phase. In the present work, we proceed to a detailed characterization of the ordered version of the model in [19] and the roughening transition it presents. Having such a thorough analysis will not only serve as grounds for our results on super-roughening [19], but will also be relevant from a much more general viewpoint, as a case study for 1D phase transitions and as an alternative way to obtain information about complicated problems in higher-dimensional systems.

Indeed, the first of the two goals above may seem questionable in view of the fact that the subject of 1D thermodynamic phase transitions, defined as nonanalyticities of the free energy, has long been excluded from the attention of the community. This exclusion comes from the "public knowl-edge" that phase transitions cannot occur in 1D systems with short-range interactions. However, this general belief has risen due to the misunderstanding of van Hove's theorem [20,21] and abuse of Landau's [22] argument about the entropic contribution of domain walls to the free energy. In fact, there are many known examples of this kind of transition (see [23] for a comprehensive study of the matter), although most of them have been hidden using language tricks that have made us speak about $1+1$ dimensions. This has been the case, for instance, with a number of models of the so-called "2D wetting" that are in fact 1D in the mathematical sense, as [24,25], just to give a couple of examples. In this sense, our work is yet another piece of detailed evidence about the existence of 1D phase transitions. In addition, our model has immediate applications, such as crystalline growth over an impenetrable substrate, or "2D wetting" favoring the formation of layers of the condensed phase. On the other hand, as mentioned in the previous paragraph, it is clear that the same approach can be used for the study of other 2D problems, which may allow the formulation of a 1D counterpart such as the one we present in this paper for the sine-Gordon model.

With the above objectives in mind, the paper is organized as follows. Section II introduces our model by discussing in detail its predecessors, the Burkhardt and the sine-Gordon ones. Subsequently, in Sec. III we present the transfer operator formalism and develop it into the pseudo-Schrödinger-equation approximation that predicts a phase transition for the model. We thus obtain analytical expressions for the magnitudes of interest at low and high temperatures. Then in Sec. IV we solve numerically the transfer operator problem, showing the existence of the phase transition and computing thermodynamical magnitudes such as the specific heat. In Sec. V, we present the results of Monte Carlo parallel tempering simulations of the model, compare them with the pre-

*Electronic address: saul@math.uc3m.es

†URL: http://gisc.uc3m.es/~saul

ceding results, and discuss the nontrivial behavior in the flat phase of the model. Finally, in Sec. VI we discuss the consequences of all this as well as further implications of our results.

II. MODEL DEFINITION

In order to properly introduce and motivate our model, we find it convenient to review in some detail the two previously proposed ones on which it is based, namely the model introduced by Burkhardt in 1981 [26] in the context of wetting, and the sine-Gordon model, a widely applicable model representative of a variety of physical systems (see [9] and references therein). Beginning with the first one, the Hamiltonian of Burkhardt's model is given by [26]

$$\mathcal{H} = \sum_{i=1}^{N} \{J|h_{i+1} - h_i| - U(h_i)\} \qquad (1)$$

and defines a continuous counterpart of the models proposed by Chui and Weeks [27] and van Leeuwen and Hilhorst [28] in 1981. We are interested in the version of the model with positive values of the variables ($h_i \geq 0$). $U(h_i)$ is a function with a positive constant value U_0 for $h_i \leq R$ and zero for $h > R$. The variables h_i can be seen as heights over a substrate (located at $h=0$), defining all together an interface. This model is exactly solvable because its transfer integral equation can be exactly mapped [26] to a Schrödinger equation, formally a quantum square well problem in 1D with the square well potential at the edge of the system. From quantum mechanics [29], we know that this potential has a bound state solution for a well deep enough. In Burkhardt's statistical mechanical problem, the depth of the well of the resulting Schrödinger equation depends on β, the inverse temperature. Hence, for low enough temperatures, the quantum bound state maps to an interface trapped by the potential, and therefore the interface is flat, in the sense that its width is finite. Above the critical temperature of the model, the bound state disappears and the interface depins from the potential and its width diverges: it becomes rough.

The other pillar on which our model stands is the 1D sine-Gordon model, whose Hamiltonian is

$$\mathcal{H} = \sum_{i=1}^{N} \left\{ \frac{J}{2}(h_{i+1} - h_i)^2 + V_0[1 - \cos(h_i)] \right\}, \qquad (2)$$

where now the values of the variables are unrestricted ($-\infty \leq h_i \leq \infty$). Its 2D version is very interesting because it can describe a number of different physical problems [9] and because it presents a *roughening* phase transition. Again in the language of h_i being the height of a surface, this transition takes place between a high-temperature rough and a low-temperature flat phase (we will define more precisely below what we understand by rough and flat). In the rough phase, the roughness (also to be defined below, but in the surface language can be thought of as the surface width) of the system scales as $\ln L$, the logarithm of the system size. The roughening transition is modified by the addition of disorder to the system: when the cosine potential is changed

adding a quenched disorder h_i^0, making it $V_0[1-\cos(h_i -h_i^0)]$, a *super-roughening* transition arises, characterized by the fact that the low-temperature phase is no longer flat. The super-roughening transition and especially the low-temperature phase are poorly understood. One of the features that seems to be accepted about this *super-rough* phase is that in it the roughness scales as $\ln^2 L$, so in this sense it would be even *rougher* than the high-temperature rough phase (hence the name super-rough). Unfortunately, the 1D version of the sine-Gordon model, much easier to study analytically and numerically, is of no help to shed light on this problem, as long as it has been rigorously proven [30] that it cannot have a true thermodynamic transition (although it does have an apparent one for any finite-size systems, even extremely large ones [31]).

In order to better understand the phenomenology of the 2D version of the model, in [19] we introduced a new model containing the features of Burkhardt's and sine-Gordon models, in order to retain the most interesting characteristics of both of them: the phase transition of the first one and the periodic potential of the latter. The rationale for this approach was that if we had a 1D model with such a phase transition, we could consider its disordered version and check whether or not it reproduces the features of 2D super-roughening. We indeed carried out this program in [19], but a key question remained, namely whether or not the basic, ordered, 1D model had a true thermodynamic phase transition or not. Only if the answer to this question is positive will the approach in [19] make sense. Although our model is specifically designed to exhibit this phase transition, and hence the transition itself would not be surprising, we must prove that the model behaves as expected: the fact that the model ingredients suggest that it will indeed have a transition by no means warrants its existence. In addition, the main purpose of this paper is the characterization of the low-temperature phase, which will show novel nontrivial behavior as we will see below.

The Hamiltonian for our model, which we called the Burkhardt–sine-Gordon model, (BSGM hereafter), is

$$\mathcal{H} = \sum_{i=1}^{N} \left\{ \frac{J}{2}(h_{i+1} - h_i)^2 + V_0 V(h_i) \right\}, \qquad (3)$$

where

$$V(x) = \begin{cases} [1 - \cos(x)] - \dfrac{1}{V_0}U(x) & \text{if } x \geq 0, \\ \infty & \text{if } x < 0. \end{cases} \qquad (4)$$

The choice for a quadratic coupling instead of an absolute value one as in [26] is to make our model as close as possible to the original sine-Gordon model. In addition, the Gaussian fluctuations of the heights that this coupling implies can be simulated with higher efficiency using a heat bath algorithm [31,32]. We impose no explicit restriction over the values of h_i; it is the value of the potential for $h_i < 0$ that forces the variable to take only positive values. This unlimited range of definition of the variable will be useful for the formal operations we will perform. We see now that $U(x)$ can be seen as

an attractive potential binding the interface to the substrate. The cosine potential will favor the growth-forming layers at a distance 2π from each other. For definiteness we choose the parameters of the model to be $V_0=1$, $U_0=2$, and $R=2\pi$. In that way, the substrate will attract the first two layers. We have also performed simulations with different values of the parameters. In that way, we can change the number of attracting layers, or the critical temperature, but no new qualitative behavior is found.

In view of the above considerations, we expect the BSGM to have a phase transition between a flat (or pinned) phase at low temperatures and a rough (or depinned) one at high temperatures. That is exactly what we needed in order to compare to the results on 2D super-roughening in disordered sine-Gordon models [19]. However, in that previous work, we did little more than provide plausibility arguments and simulation evidence for the existence of such a transition, hence the necessity of the detailed, much more rigorous work presented here. To characterize the transition, we define the roughness or interface width, w, as

$$w^2 = \left\langle \frac{1}{N} \sum_{i=1}^{N} [h_i - \bar{h}]^2 \right\rangle, \tag{5}$$

where

$$\bar{h} \equiv \frac{1}{N} \sum_{i=1}^{N} h_i \tag{6}$$

is the mean height, and averages $\langle \cdots \rangle$ are to be understood with respect to a statistical weight given by the Gibbs factor, $e^{-\mathcal{H}/T}$, at equilibrium at a temperature T. Then we say that an interface is flat when w is finite and does not depend on the system size, N. In the rough phase, the interface width grows with N and diverges in the thermodynamic limit, $w \to \infty$ as $N \to \infty$. Additionally, in the remainder of the paper we will look at other possible indicators of the transition, such as the free energy, the specific heat, or the full correlation function.

III. ANALYTICAL RESULTS

A. Transfer integral technique

The following discussion of the transfer integral (TI) technique follows that in [33] for the sine-Gordon model. The classical canonical partition function of the BSGM [Eq. (3)] can be written as

$$\mathcal{Z}_N(\beta) = \int_{-\infty}^{\infty} dh_1 \int_{-\infty}^{\infty} dh_2 \cdots \int_{-\infty}^{\infty} dh_N e^{-\beta \mathcal{H}}, \tag{7}$$

β being the inverse temperature in units of the Boltzmann constant. Note that we could have written the integrals in the range $[0, \infty)$, but our definition of $V(h_i)$ makes this unnecessary. In what follows, periodic boundary conditions

$$h_1 = h_{N+1} \tag{8}$$

are assumed, so that Eq. (7) can be replaced by

$$\mathcal{Z}_N(\beta) = \int_{-\infty}^{\infty} dh_1 \cdots \int_{-\infty}^{\infty} dh_{N+1} e^{-\beta \mathcal{H}} \delta(h_1 - h_{N+1}). \tag{9}$$

To evaluate $\mathcal{Z}_N(\beta)$, we proceed as follows. The δ function is represented as an expansion in a set of complete orthonormal functions $\varphi_n(h)$,

$$\delta(h - h') = \sum_n \varphi_n^*(h) \varphi_n(h'). \tag{10}$$

The functions φ_n are chosen to satisfy the TI equation,

$$\int_{-\infty}^{\infty} dh \exp[-\beta V_0 K(h, h')] \varphi_n(h) = \exp(-\beta V_0 \epsilon_n) \varphi_n(h'), \tag{11}$$

where

$$K(h, h') = \frac{1}{2} \frac{J}{V_0} (h - h')^2 + \frac{1}{2}[V(h) + V(h')], \tag{12}$$

φ_n is an eigenfunction of the TI equation with associated eigenvalue $\exp(-\beta V_0 \epsilon_n)$, and

$$\mathcal{T}(\beta) = \exp[-\beta V_0 K(h, h')] \tag{13}$$

is the transfer operator of the model. Using this, we can rewrite the partition function,

$$\mathcal{Z}_N(\beta) = \sum_n \exp(-\beta V_0 \epsilon_n N) \int_{-\infty}^{\infty} dh \varphi_n^*(h) \varphi_n(h)$$

$$= \sum_n \exp(-\beta V_0 \epsilon_n N). \tag{14}$$

In the last step, we have used the orthonormality of the φ_n. The orthogonality and completeness of the eigenfunctions are guaranteed by the Sturm-Liouville theory for Fredholm integral equations with a symmetric kernel [34], for which Eq. (12) is an example.

Since the single-site potential [Eq. (4)] is bounded from below, the eigenspectrum is also bounded from below, and we denote the lowest eigenvalue by ϵ_0. This corresponds to $\exp(-\beta \epsilon_0)$, the maximum eigenvalue of the transfer operator (13). In the thermodynamic limit, the free energy per particle is then given by

$$f = -k_B T \lim_{N \to \infty} \frac{1}{N} \ln \mathcal{Z}_N(\beta) = V_0 \epsilon_0. \tag{15}$$

From this result, other thermodynamic properties can now be derived, i.e., internal energy per particle

$$e = \frac{1}{N} \langle \mathcal{H} \rangle = f - T \frac{\partial f}{\partial T} \tag{16}$$

and specific heat at constant volume (length)

$$c_V = \frac{\partial e}{\partial T} = -T \frac{\partial^2 f}{\partial T^2}. \tag{17}$$

In [33], it is also shown that in the thermodynamic limit canonical averages are given by the expression

$$\langle g(h_i) \rangle = \int_{-\infty}^{\infty} |\varphi_0(h)|^2 g(h) dh, \tag{18}$$

which means that $|\varphi_0(h)|^2$ can be understood as the probability density for the variables h_i.

We have been unable to exactly evaluate the free energy (15) for the BSGM [Eq. (3)]. As an alternative, in this work we will proceed in two different ways: through the pseudo-Schrödinger-equation approximation associated to the TI equation and computing numerically the eigenvalues of the transfer operator. In what follows, we discuss the former approach as well as the approximate analytical results that can be obtained from it. The numerical study of the full transfer operator deserves a separate treatment and is reported in Sec. IV.

B. Pseudo-Schrödinger equation

Defining

$$\psi_n(h) = \exp\left[-\beta V_0 \frac{1}{2} V(h)\right] \varphi_n(h) \tag{19}$$

and using the identity

$$\frac{1}{\sqrt{2\pi t}} \int_{-\infty}^{\infty} dy \left[\exp\left(-\frac{1}{2t}(x-y)^2\right)\right] f(y) = \exp\left(\frac{t}{2}\frac{d^2}{dx^2}\right) f(x), \tag{20}$$

the TI equation (11) may be rewritten in the form

$$\exp\left(\frac{1}{2\beta}\frac{1}{\sqrt{V_0 J}}\sqrt{\frac{V_0}{J}}\frac{d^2}{dh^2}\right)\psi_n(h)$$

$$= \exp\left[-\beta\sqrt{V_0 J}\sqrt{\frac{V_0}{J}}[\epsilon_n - V_{eq} - V(h)]\right]\psi_n(h), \tag{21}$$

where

$$V_{eq} = \frac{1}{2V_0\beta}\ln\left(\frac{\beta J}{2\pi}\right). \tag{22}$$

In the limit of strong coupling ($J/V_0 \to \infty$ as we keep $V_0 J$ constant, see [33] for details; it can also be understood as a continuum limit if we include the lattice constant as an explicit parameter of the model), this equation can be expanded to obtain, to first order in V_0/J,

$$\left[-\frac{1}{2\beta^2 V_0 J}\frac{d^2}{dh^2} + V(h)\right]\psi_n(h) = (\epsilon_n - V_{eq})\psi_n(h). \tag{23}$$

This is the Schrödinger equation for a square well with a superimposed cosine potential. The square well alone is exactly solvable, and for low values of V_0 the cosine term can be treated with perturbation theory. Equation (21) is already an approximation for our model; from Eq. (20) we can see that it is valid when $\sqrt{V_0/J} \ll \beta$ and $\sqrt{V_0/J} \ll 1/\beta$. If we take Boltzmann's constant as unity, the predictions of this equation are expected to hold quantitatively only in the the temperature region $\sqrt{V_0/J} \ll T \ll 1/\sqrt{V_0/J}$. For this interval to make sense, $\sqrt{V_0/J}$ has to be small enough. For instance, for the values of the parameters we use ($J=1, V_0=1$), there is no

temperature where the pseudo-Schrödinger equation is quantitatively accurate. However, the qualitative picture this equation yields is completely valid and describes correctly the phenomenology of the model. In the quantum-mechanical problem, for some values of the parameters of the model we have a bound state that disappears as we change the parameters. In our statistical mechanical problem, fixing all the parameters except the temperature will give us a thermodynamical phase transition between a flat phase at low temperatures, pinned by the square well potential, and a rough phase at high temperatures, where the interface has detached itself from the substrate's attraction. This is the same scenario Burkhardt found in [26]; the change of the absolute value coupling for the quadratic one and the addition of the cosine potential modify the quantitative aspects of the phase transition, but not the qualitative ones. Of course, these new features in our model will give rise to new phenomena in the flat phase's behavior. Anyway, if we make a further rough approximation and dismiss the sinusoidal part of the potential in Eq. (23), we are left with exactly the Schrödinger equation of a semi-infinite square well. From elementary quantum mechanics [29] (see also [26] for the application to Burkhardt's model), we know that the spectrum of this equation presents a continuum of scattering states. For appropriate values of the parameters (that in the statistical mechanical problem means $T < T_c$), there are one or more bound states. As $T \to T_c^-$, the gap between the strongest bound state and the first scattering state varies as

$$\Delta\epsilon \propto (T_c - T)^2. \tag{24}$$

The quadratic temperature dependence of the gap in Eq. (24) is responsible for the finite jump in the specific heat of the model. We will find this in the computation of the specific heat both from the numerical transfer operator and from Monte Carlo simulations. In Fig. 3, we show the gap between the two first eigenvalues computed from the exact numerical transfer operator; the quadratic behavior predicted in Eq. (24) is evident as $T \to Tc^-$.

For the rest of this work, without loss of generality, we will take the coupling constant $J=1$. We can do this because the effect of changing J can be taken into account rescaling V_0, U_0 and the temperature (and also the time scale, but in this work we will deal only with equilibrium properties).

C. Low- and high-temperature approximations

For low enough temperatures, it is a good approximation to suppose that all the heights fall inside the square well potential. For a value of the width of the well of $R=2\pi$, inside the well there exist two minima of the cosine potential. In that case, it is reasonable to approximate the potential by a ϕ^4 one, see Fig. 1. The good features of this choice are that the ϕ^4 potential reproduces the two-potential minima and that it bounds the system to them, as it grows to ∞ as $h \to \pm\infty$. Note that if we restrict ourselves to only one minima of the cosine potential, a parabolic potential will be enough to reproduce the leading term. To mimic the potential in our problem, this ϕ^4 potential has the form (for $V_0=1$ and $U_0=2$)
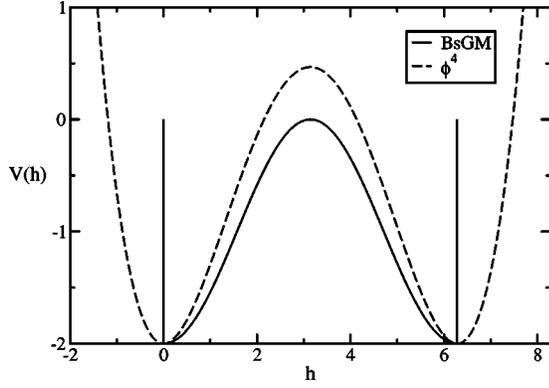
FIG. 1. Approximation of the potential inside the square well by a ϕ^4 potential. The continuous line is the BSGM potential between 0 and 2π. The dashed line is the ϕ^4 potential we use to approximate it.

$$V_{\phi^4}(h) = \frac{(h-\pi)^4}{4\pi^2} - \frac{(h-\pi)^2}{2} + \frac{\pi^2}{4} - 2. \qquad (25)$$

In [33], we find values for some thermodynamic properties of a low-temperature expansion of the ϕ^4 model. Thus, we have for the internal energy

$$e = \frac{T}{2} + \frac{36T^2}{15 \times 2^3 \pi^2}, \qquad (26)$$

and for the specific heat

$$c_V = \frac{1}{2} + \frac{72T}{15 \times 2^3 \pi^2}. \qquad (27)$$

We will see that, at low temperatures, the system chooses to be in one single potential minimum of the two displayed in Fig. 1. In fact, this assumption is implicit in the calculation that leads to Eqs. (26) and (27) (see [33] for details). This calculation approximates the ϕ^4 potential by a parabolic one $[V(h) = V_0 h^2]$, and then introduces the higher-order corrections.

The same procedure can be used with the sine-Gordon model instead of the ϕ^4 model. It also seems a reasonable choice to approximate the $T \rightarrow 0$ regime using this potential. In the end, as both models have the same leading term, the differences between them will be small. We will compare the expressions arising from both of them with the results of our simulations, and find that both of them describe remarkably well physical magnitudes when $T \rightarrow 0$. From [33], we have the following expressions for the low-temperature sine-Gordon model:

$$e = \frac{T}{2} + 2\left[\left(\frac{T}{8}\right)^2 + \left(\frac{T}{8}\right)^3 + \cdots\right], \qquad (28)$$

$$c_V = \frac{1}{2} + 2\left[\frac{2T}{8^2} + \frac{3T^2}{8^3} + \cdots\right]. \qquad (29)$$

Both these approximations suppose the system is trapped in a single well of the potential, and it can be seen that this implies that the system is in a flat phase [31]. So agreement with these results is a signal of a flat phase.

Restricting ourselves to the lowest-order approximation for vanishing temperatures, that is, a flat system trapped in a single parabolic potential, it is straightforward to calculate the roughness and correlation functions, as was done in [31]. The parameter of the parabolic potential has to be $V_0 + U_0$. For the roughness we obtain

$$w^2(T) = \frac{T}{\sqrt{(2+V_0+U_0)^2 - 4}}. \qquad (30)$$

We define the height-difference correlation function as

$$C(r) = \left\langle \frac{1}{N} \sum_j [h_j - h_{j+r}]^2 \right\rangle. \qquad (31)$$

It can be shown that the parabolic potential approximation yields for it

$$C(r) = \frac{2T}{\sqrt{(2+V_0+U_0)^2 - 4}} [1 - C_c(r)], \qquad (32)$$

where

$$C_c(r) = \left\{ \left(1 + \frac{V_0+U_0}{2}\right) \left[1 - \sqrt{1 - \left(\frac{2}{2+V_0+U_0}\right)^2}\right] \right\}^r. \qquad (33)$$

In the asymptotic limit $r \rightarrow \infty$, $C_c(r) \rightarrow 0$, and we have that $C(\infty) = 2w^2$.

In the high-temperature phase, the potential effectively vanishes and we are left with the quadratic coupling alone: this is the Edwards-Wilkinson model [35]. The predictions for the internal energy ($e = T/2 + \text{const}$) and the specific heat ($c_V = 1/2$) are expected to hold in the rough phase of our model. However, the prediction for the interface width is not so accurate: the existence in our model of an impenetrable substrate changes the statistics of the rough interface.

IV. NUMERICAL TRANSFER OPERATOR RESULTS

The eigenvalue problem in Eq. (11) can be solved discretizing the transfer operator in Eq. (13) and evaluating numerically the eigenvalues of the resulting matrix (see [33,36,37]; see [38] for a detailed account). The relevant parameters of the discretization of the operator are Δh, the discretization length, and M, the number of points considered, that is, the size of the matrix. From them we obtain immediately the interval where the discretized variable takes values, $[0, h_{max}]$, where $h_{max} = (M-1)\Delta h$. The two sources of error of this numerical procedure are the discretization of the real variable h and the cutoff of the variable range at h_{max}. In the limit $\Delta h \rightarrow 0$ and $M\Delta h \rightarrow \infty$ (that is, $h_{max} \rightarrow \infty$), this numerical approach is exact.

A thermodynamic phase transition takes place when there is a nonanalyticity in the free energy. We have seen in Eq. (15) that in the thermodynamic limit, the free energy is de-
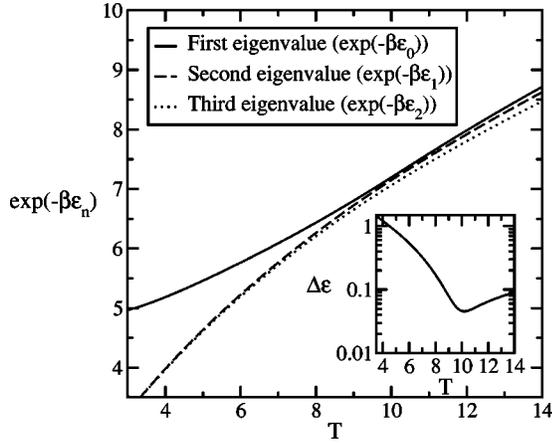
FIG. 2. Three first eigenvalues for $M=4096$ and $\Delta h=1/32$. Inset: Difference $\Delta\epsilon=\exp(-\beta\epsilon_0)-\exp(-\beta\epsilon_1)$ vs T. The minimum gives the temperature of the phase transition.

termined by the largest eigenvalue of the transfer matrix. As discussed below Eq. (24), the vanishing of the gap between the largest two eigenvalues leads to a singularity. To find the point of a phase transition, we have to find a minimum of the gap and show that the minimum goes to zero as we increase M.

In Fig. 2, we show the first three eigenvalues of the discretized transfer operator with our standard set of parameters, $V_0=1$, $U_0=2$, and $R=2\pi$. We clearly see that the first two eigenvalues become very close near $T\approx 10$. In the inset, we show the minimum of $\Delta\epsilon$ that indicates the temperature of the candidate transition. The slope of ϵ_0 does not change discontinuously at T_m, the temperature of the minimum, so the transition will be continuous and not first order.

In Fig. 3, we show the gap between the two first eigenvalues for a range of matrix sizes, keeping Δh fixed. We see that as M increases, the minimum value of the gap becomes closer to zero. In Figs. 4 and 5, we perform a finite-size
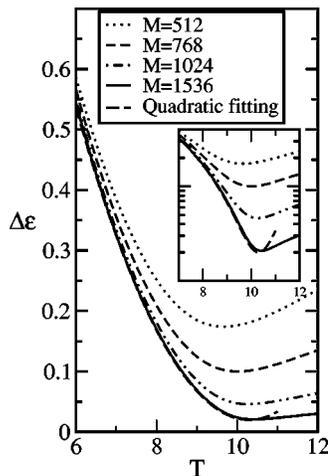

FIG. 3. $\Delta\epsilon$ for different matrix sizes as indicated in the plot. The discretization is $\Delta h=1/8$. Inset: the same figure with the $\Delta\epsilon$ axis in logarithmic scale. We see that as M becomes greater, $\Delta\epsilon$ goes quadratically to its minimum as $T\rightarrow T_c^-$, as shown for $M=1536$ using a quadratic fit. This is exactly the prediction of Eq. (24).
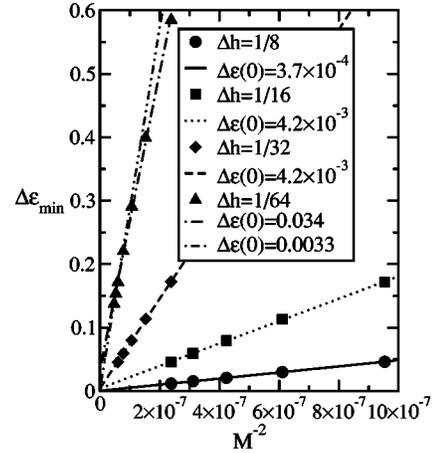

FIG. 4. Minimum value of the gap for different discretization values and matrix sizes, as indicated in the plot.

scaling to check that the minimum of the gap, $\Delta\epsilon_{min}$, goes to zero, and how the different temperatures for the minimum go to the critical temperature, T_c. We see, as observed in [36] for a different model, that both $\Delta\epsilon_{min}$ and T_m scale with M^{-2} when we change M keeping Δh fixed. Of course, this scaling is supposed to improve for greater matrix sizes, and this aspect is important especially for small Δh. In Fig. 4, we see how as M increases, $\Delta\epsilon_{min}$ goes to zero. It may seem contradictory that as we take a better (smaller) Δh, the convergence to zero becomes worse. The explanation comes from the fact that, as we use a smaller Δh, we need a bigger M to get a correct scaling. However, memory limitations of our computers set a limit to the values of M we can use: we cannot go much further than $M=4096$ in a reasonable amount of time. So, to get a better estimation of $\Delta\epsilon_{min}$, we use only the points with the best scaling. That is what we do for $\Delta h=1/64$, where using only the two points of greater M, we see that the asymptotic value is corrected in one order of magnitude. We can then safely expect $\Delta\epsilon_{min}\rightarrow 0$ as $M^{-2}\rightarrow 0$ and $\Delta h\rightarrow 0$. This means that in fact we have a true thermodynamic phase transition, as predicted by the pseudo-Schrödinger approximation. The critical temperature T_c can be inferred from the data in Fig. 5. The data coming from the smallest values of Δh are supposed to be the best ones, and again we have used
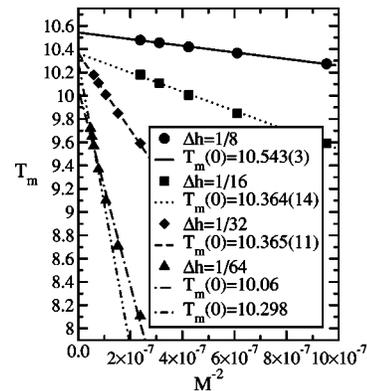

FIG. 5. Critical temperature for different discretization values and matrix sizes as indicated in the plot.
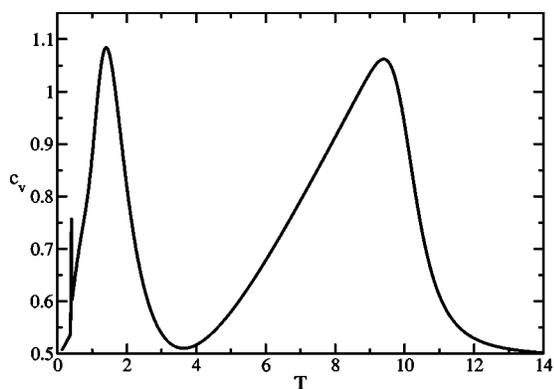
FIG. 6. Specific heat as a function of temperature obtained from the discretized transfer operator for $\Delta h = 1/32$ and $M = 4096$.

only the last two values for $\Delta h = 1/64$ to correct the effects of the lack of scaling for low M. With the data in the figure, we can estimate the critical temperature as $T_c = 10.3$ in our units.

We have also computed, using Eq. (17), the specific heat from the numerically obtained eigenvalue. This is shown in Fig. 6. The jump of the specific heat at $T \approx 10.3$ is the jump associated with the phase transition. The peak at $T \approx 1.4$ is a well-known Schottky anomaly (see, e.g., [9] and references therein) related to the fact that the heights pass from being mostly in one well of the cosine potential to expand to different wells. There is an extra feature, namely the narrow peak at $T \approx 0.4$. If we look at the gap $\Delta\epsilon$ between the two first eigenvalues, it effectively has a minimum at that temperature, which would make us think of an additional phase transition. Furthermore, that transition would have a physical interpretation. In Fig. 7, we represent the square value of the first eigenvalue of the transfer operator, which as we saw in Eq. (18) has the interpretation of the probability density of h_i. In the figure, we see that at the temperature of the transition ($T \approx 0.77$ for the parameters of the figure) the heights pass from being almost all in the lowest h well of the cosine potential (the potential well with the minimum at $h=0$) to being in the highest h one (the well with minimum at $h = 2\pi$). This "transition," however, does not survive a finite-

size study: as, keeping h_{max} fixed, we make Δh smaller, the temperature of the transition goes to zero, showing us that it is nothing but a result of the discretization and the numerical technique employed. Our Monte Carlo simulations will confirm this, as they show all the way down to the lowest temperature we have simulated, below $T = 0.1$, that the well preferred by the heights is the highest h one (see Sec. V and Fig. 12 below). Upon this observation, one question immediately arises: if both the first and the second well of the cosine potential are energetically equally favorable, why does the system choose as the equilibrium one the second? The reason is that entropically they are not the same, and the configuration of the heights in the highest h well has greater entropy. The reason for this is that the only escape a height h_i has from the lowest h well is going to the highest h one (at low enough temperatures at which big h differences are very unlikely). But from the highest h well, it can escape to the lowest h one, or to the next cosine well outside the Burkhardt-like square well. So the two wells are not symmetrical, and the configurations in the highest h one have higher entropy. In that way, what we see in the lowest-temperature curves in Fig. 7 would be in fact a metastable state with higher free energy than the true equilibrium one, the heights in the highest h well.

V. MONTE CARLO SIMULATIONS

To confirm the conclusions drawn from the analytical simulations on the existence of a phase transition, we have resorted to parallel tempering Monte Carlo simulations [31,39,40]. Representative configurations at a given temperature are generated with a heat bath algorithm [31,32], in which new values h_i' for the height at site i are proposed according to the rule

$$h_i' = \frac{h_{i-1} + h_{i+1}}{2} + \xi\sqrt{\frac{T}{2J}}, \qquad (34)$$

ξ being a Gaussian random variable of zero mean and unit variance, and are accepted with a probability $\min[1, e^{-\delta\mathcal{H}/T}]$ with $\delta\mathcal{H} = [V(h_i') - V(h_i)]$. The reason to accept or reject using only the potential term in the Hamiltonian is that the proposal in Eq. (34) *exactly* reproduces the quadratic coupling fluctuations, which are Gaussian. Since that term is already fully included in the proposal, we do not need it in the acceptance rate.

The parallel tempering algorithm then considers simultaneous copies of the system at different temperatures, allowing exchange of configurations between them. This is particularly efficient for low-temperature configurations, which are most susceptible to being trapped in metastable regions. The simulation starts using a single system copy (replica) at the highest temperature of interest. After simulating it, we get the temperature for the next replica from the energy fluctuations. We repeat the same process until we have a set of temperatures that covers the whole range of interest. Then we run a parallel tempering simulation of all replicas and from it get improved values of the temperature set. This autotuning process continues until we have an almost perfect
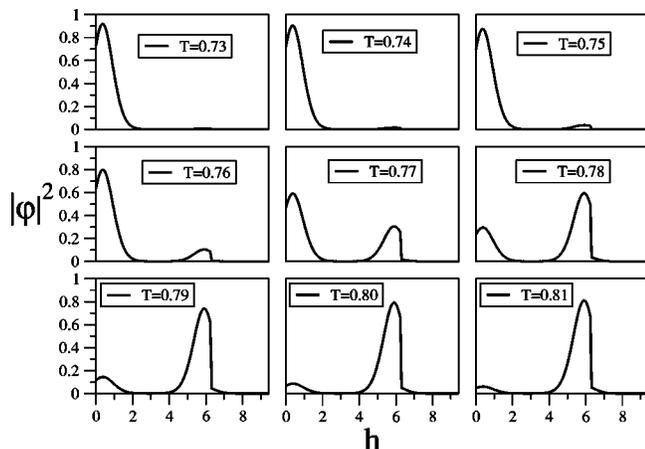

FIG. 7. Probability density of h for different temperatures around the narrow peak of the specific heat for $M = 1440$ and $h_{max} = 100$ ($\Delta h = 5/72$).
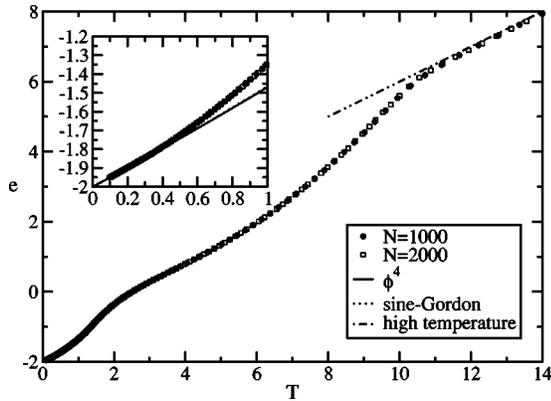
FIG. 8. Internal energy per particle obtained from Monte Carlo simulations. Inset: display of the low-temperature region and comparison with the predictions of Eqs. (26) and (28). Note that the zero-temperature energy is shifted by −2 with respect to Eqs. (26) and (28) to take into account the square-well potential. Lines are as indicated in the plot. At this scale, the predictions of the sine-Gordon and the ϕ^4 models (in the inset) are indistinguishable.

measure of the specific heat, which shows that we are using a near to optimal temperature set, and at the same time that the different replicas are properly equilibrated. After allowing this last temperature set replicas run for further equilibration, we start the measuring run.

The parameters we have used for our simulations, as already said, are $V_0=1$, $U_0=2$, and $R=2\pi$. We also ran simulations with different values of the parameters without finding qualitative differences. We have made simulations for system sizes of $N=500$, $N=1000$, and $N=2000$, although for simplicity we do not present results for $N=500$. In Fig. 8 we plot the internal energy per particle. We see that the results for both system sizes agree perfectly, and that the agreement with the theoretical predictions for low temperature [Eqs. (26) and (28)] is quite remarkable. At high temperature it has the predicted slope 0.5, and we see at $T \simeq 10$ the change in the slope indicating the temperature of the phase transition. Figure 9 shows the specific heat obtained from the simulations. We see that the coincidence between both system sizes
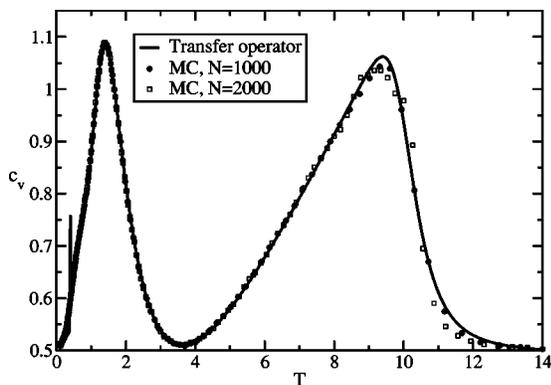

FIG. 9. Specific heat from Monte Carlo simulations; comparison is made with the numerical transfer operator result. Error bars of the simulations are of the size of the symbols or smaller. Symbols and lines are as indicated in the plot.
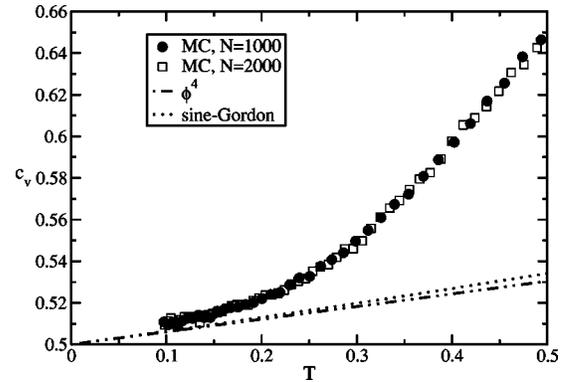

FIG. 10. Specific heat from Monte Carlo simulations at low temperatures compared with the predictions of Eqs. (27) and (29). The symbols are simulation results for different system sizes as indicated in the plot. Error bars are of the size of the symbols. The dashed–double-dotted line is the prediction of Eq. (27) and the dotted one is the prediction of Eq. (29).

and the numerical transfer operator result is perfect, except in the low-temperature region, where we have seen that the numerical transfer operator introduces the spurious transition, and in the region of the phase transition, where small discrepancies due to finite-size effects arise. As should be expected, the transition is more abrupt for the largest system size, $N=2000$. This agreement between the results of two completely different approaches—the numerical transfer operator and the Monte Carlo simulations—provides firm grounds to our claims. In Fig. 10, we see how the specific heat has an asymptotic behavior as $T \to 0$, in agreement with approximations (27) and (29).

As the most important verification of the transition, Fig. 11 shows the squared roughness. For temperatures above the phase transition, w^2 becomes dependent on the system size and diverges with N, showing us that we are in a rough phase. Below T_c, the results for both system sizes are the same, and as $T \to 0$ we see the behavior predicted in Eq. (30). The step in the roughness between $T \simeq 1$ and $T \simeq 1.5$ is an
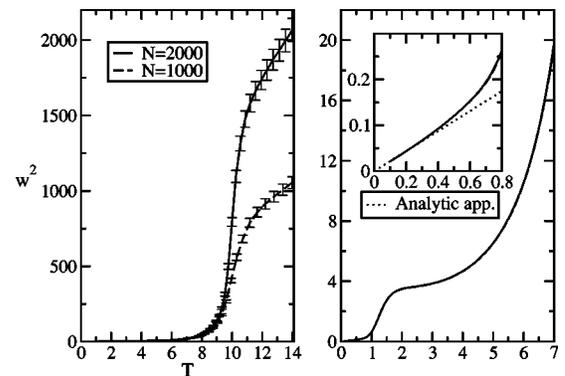

FIG. 11. Left: squared roughness w^2 vs T. Right: zoom of a lower-temperature region. Note the perfect overlap of the results for the two different system sizes below the transition temperature. Inset: yet another zoom of an even lower-temperature region, where we can see the comparison between simulation results and the prediction of Eq. (30).
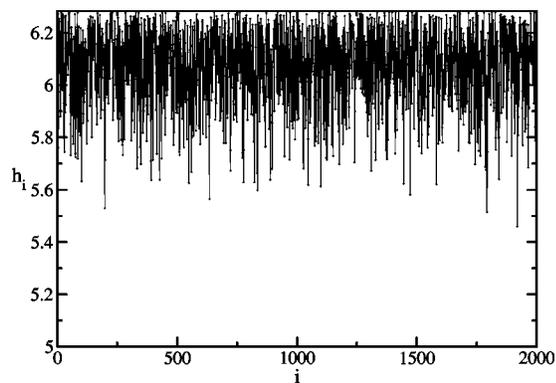
FIG. 12. Typical interface configuration at low temperatures. This one is for the $N=2000$ Monte Carlo simulation at $T=0.0981$.

effect of the Schottky anomaly [31] we have already mentioned. Between $T \simeq 2$ and $T \simeq 4$, we see a little plateau in the roughness curve. This plateau is caused by the dominating part that the kinks formed between the lowest h well and the highest h one play at these temperatures, while the relaxation of the heights in each well as temperature goes down is almost screened by the effect of the kinks in the roughness. At the lowest temperatures, below $T \simeq 1$, all effects of kinks disappear, and the interface is trapped in the highest h well in the square potential, as we already noted above and shown in Fig. 12. This is related to the apparent phase transition studied in [31].

In Fig. 13, we see the height-difference correlation function, scaled by temperature, from the simulations with $N = 2000$. All the curves corresponding to temperatures higher than T_c collapse to a single curve. This is the expected behavior for the high-temperature rough phase, as the potential term in the Hamiltonian is expected to be irrelevant at these temperatures, leaving us only with the quadratic coupling, which is the Edwards-Wilkinson model [35] that predicts exactly this independence of T for $C(r)/T$, see also [9]. The first curve below this collapse is the curve for $T=10.26$. So, from our simulations we obtain $T_c=10.26$, in excellent agreement with the numerical transfer operator result. For $N = 1000$ (not shown), we obtain $T_c=10.31$ and the same behavior depicted in Fig. 13. Finally, note the agreement between the prediction of Eq. (32) and the actual low-temperature correlation functions we find in simulations. We see again in Fig. 13 the effect of kinks that appeared in the roughness between $T \simeq 2$ and $T \simeq 4$: the temperature scaled height-difference correlation function has a nonmonotonous behavior with temperature between $T=3.99$ and $T=1.62$. In this range, the different functions (without scaling) are almost independent of temperature, so the scaled functions have higher values as we reduce temperature. Note that this behavior only appears above certain length scale. At very short scales, the effect of kinks has little importance (as we need a certain system size to have probabilities of kinks to appear) and the relaxation of heights continues with decreasing temperature.

VI. CONCLUSIONS

We have studied in detail a model first proposed by us [19], which combines the model proposed by Burkhardt in [26] and the well known sine-Gordon model. We show here by analytic approximations and by two different numerical methods (transfer operator and Monte Carlo simulation) that it has a continuous phase transition between a high-temperature rough phase and a low-temperature flat one. We have characterized the thermodynamics of the model, establishing its nontrivial behavior in the flat phase due to interaction of the two kinds of forces (periodic potential and substrate attraction) present in it. This gives rise to the existence of a temperature region (between $T \simeq 1.6$ and $T \simeq 4.0$) where physical magnitudes of the interface as roughness and spatial correlations are quite independent of the temperature. In addition, our work also stands as a careful study of a 1D thermodynamical phase transition. While we hope our results will stimulate further studies in this field, misunderstood for a long time, we want to add a few caveats about how numerical results can lead to misleading conclusions. First, we have seen that the numerical analysis of the transfer operator produced an artifact which looked like a second phase transition in the low-temperature regime. Second, we have shown in a previous paper [31] that simulations can yield results reminiscent of a true phase transition even for extremely large system sizes, whereas it is rigorously known [30] that such a transition is impossible. Therefore, it must be borne in mind that only a judicious combination of theoretical results, numerical analysis, and simulations may provide firm grounds for claims of the existence of phase transitions in models that are not exactly solvable. This is even more important in the case of 1D systems, where the debate is contaminated by the false prejudices against their own existence [23].

Finally, we want to stress that the results we have obtained for this model suggest a more amenable analytical and computational way to study the properties of modified versions of the 2D sine-Gordon model, as we did in [19] for the random substrate version. As our model has a transition between a low-temperature flat phase and a high-temperature rough one, just like the 2D sine-Gordon model without disorder, in that work we showed how the addition of disorder
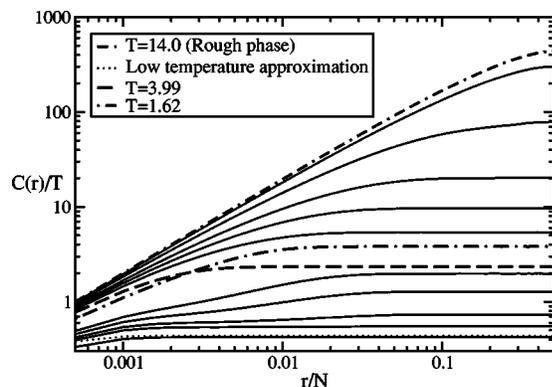

FIG. 13. Height difference correlation functions scaled by the temperature from the $N=2000$ simulation. Temperatures are (from up to down of the greatest value: $T=14.0$, 10.26, 9.53, 8.56, 7.80, 6.90, 1.62, 3.99, 1.12, 0.995, 0.836, 0.697, 0.0981).

to our model can give us insight into what happens in the low-temperature phase of the 2D random sine-Gordon model. We believe that the same 1D approach to 2D problems will prove fruitful in many other contexts. Its two main advantages are that usually 1D models are more amenable to analytical treatment than 2D ones, and that simulating a 1D model requires much less computational effort. We hope that many new insights will be obtained following this line of research.

[1] M. Plischke and B. Bergersen, *Equilibrium Statistical Physics* (World Scientific, Singapore, 1994), Chap. 11 and references therein.

[2] J. D. Weeks and G. H. Gilmer, Adv. Chem. Phys. **40**, 157 (1979); J. D. Weeks, in *Ordering in Strongly Fluctuating Condensed Matter Systems*, edited by T. Riste (Plenum, New York, 1980).

[3] H. van Beijeren and I. Nolden, in *Structure and Dynamics of Surfaces*, edited by W. Schommers and P. von Blackenhagen, Topics in Current Physics Vol. 43 (Springer, Berlin, 1987).

[4] A. L. Barabási and H. E. Stanley, *Fractal Concepts in Surface Growth* (Cambridge University Press, Cambridge, 1995).

[5] J. Krug, Adv. Phys. **46**, 139 (1997).

[6] A. Pimpinelli and J. Villain, *Physics of Crystal Growth* (Cambridge University Press, Cambridge, 1998).

[7] J. Toner and D. P. DiVincenzo, Phys. Rev. B **41**, 632 (1990).

[8] Y. Shapir, in *Dynamics of Fluctuating Interfaces and Related Phenomena*, edited by D. Kim, H. Park, and B. Kahng (World Scientific, Singapore, 1997).

[9] A. Sánchez, A. R. Bishop, and E. Moro, Phys. Rev. E **62**, 3219 (2000).

[10] H. Rieger, Phys. Rev. Lett. **74**, 4964 (1995).

[11] E. Marinari, R. Monasson, and J. J. Ruiz-Lorenzo, J. Phys. A **28**, 3975 (1995).

[12] D. J. Lancaster and J. J. Ruiz-Lorenzo, J. Phys. A **28**, L577 (1995).

[13] C. Zeng, A. A. Middleton, and Y. Shapir, Phys. Rev. Lett. **77**, 3204 (1996).

[14] U. Blasum, W. Hochstättler, U. Moll, and H. Rieger, J. Phys. A **29**, L459 (1996); H. Rieger and U. Blasum, Phys. Rev. B **55**, R7394 (1997).

[15] B. Coluzzi, E. Marinari, and J. J. Ruiz-Lorenzo, J. Phys. A **30**, 3771 (1997).

[16] A. Sánchez, A. R. Bishop, D. Cai, N. Grønbech-Jensen, and F. Domínguez-Adame, Physica D **107**, 325 (1997).

[17] J. J. Ruiz-Lorenzo, in *Proceedings of the VIII Spanish Meeting on Statistical Physics FISES '97*, edited by J. A. Cuesta and A. Sánchez (Editorial del Ciemat, Madrid, 1998).

[18] H. Rieger, Phys. Rev. Lett. **81**, 4488 (1998).

[19] S. Ares, A. Sánchez, and A. R. Bishop, Europhys. Lett. **66**, 552 (2004).

[20] L. van Hove, Physica (Amsterdam) **16**, 137 (1950) (reprinted in [21], p. 28).

[21] *Mathematical Physics in One Dimension*, edited by E. H. Lieb and D. C. Mattis (Academic, New York, 1966).

[22] L. D. Landau and E. M. Lifshitz, *Statistical Physics Part 1* (Pergamon, New York, 1980).

[23] J. A. Cuesta and A. Sánchez, J. Stat. Phys. **115**, 869 (2004).

[24] G. Forgacs, J. M. Luck, Th. M. Nieuwenhuizen, and H. Orland, Phys. Rev. Lett. **57**, 2184 (1986).

[25] B. Derrida, V. Hakim, and J. Vannimenus, J. Stat. Phys. **66**, 1189 (1992).

[26] T. W. Burkhardt, J. Phys. A **14**, L63 (1981).

[27] S. T. Chui and J. D. Weeks, Phys. Rev. B **23**, R2438 (1981).

[28] J. M. J. van Leeuwen and H. J. Hilhorst, Physica A **107**, 319 (1981).

[29] L. I. Schiff, *Quantum Mechanics*, 2nd ed. (McGraw-Hill, New York, 1968).

[30] J. A. Cuesta and A. Sánchez, J. Phys. A **35**, 2377 (2002).

[31] S. Ares, J. A. Cuesta, A. Sánchez, and R. Toral, Phys. Rev. E **67**, 046108 (2003).

[32] R. Toral, in *Proceedings of the Third Granada Lectures in Computational Physics*, edited by P. L. Garrido and J. Marro, Lecture Notes in Physics Vol. 448 (Springer-Verlag, Berlin, 1994).

[33] T. Schneider and E. Stoll, Phys. Rev. B **22**, 5317 (1980).

[34] R. Courant and D. Hilbert, *Methods of Mathematical Physics Vol. I* (Wiley Classics, New York, 1989).

[35] S. F. Edwards and D. R. Wilkinson, Proc. R. Soc. London, Ser. A **381**, 17 (1982).

[36] N. Theodorakopoulos, Phys. Rev. E **68**, 026109 (2003).

[37] T. Dauxois and M. Peyrard, Phys. Rev. E **51** 4027 (1995); T. Dauxois, N. Theodorakopoulos, and M. Peyrard, J. Stat. Phys. **107**, 869 (2002).

[38] T. Dauxois, Ph.D thesis, University of Dijon, 1993.

[39] M. E. J. Newman and G. T. Barkema, *Monte Carlo Methods in Statistical Physics* (Oxford University, Oxford, 1999).

[40] Y. Iba, Int. J. Mod. Phys. C **12**, 623 (2001).